Extracellular Calcium as a Candidate Mediator of Prostate Cancer Skeletal Metastasis

Jinhui Liao,[1] Abraham Schneider,[3] Nabanita S. Datta,[1] and Laurie K. McCauley[1,2]

[1]Department of Periodontics and Oral Medicine, School of Dentistry, and [2]Department of Pathology, Medical School, University of Michigan, Ann Arbor, Michigan; and [3]Department of Diagnostic Sciences and Pathology, University of Maryland, Baltimore College of Dental Surgery, Dental School, Baltimore, Maryland

Abstract

Prostate cancer almost exclusively metastasizes to skeletal sites, indicating that the bone provides a favorable microenvironment for its localization and progression. A natural yet understudied factor in bone that could facilitate tumor localization is elevated extracellular calcium ($[Ca^{2+}]o$). The present study found that elevated $[Ca^{2+}]o$ (2.5 mmol/L) enhanced proliferation of skeletal metastatic prostate cell lines (PC-3 and C4-2B), but not the nonskeletal metastatic, epithelial-derived prostate cell line LNCaP. The proliferative effect of elevated $[Ca^{2+}]o$ was associated with higher expression of the calcium-sensing receptor (CaSR), a heterotrimeric G-protein–coupled receptor that is the predominant cell-surface sensor for $[Ca^{2+}]o$. Knockdown of the CaSR via RNA interference reduced cell proliferation *in vitro* and metastatic progression *in vivo*. CaSR signaling in PC-3 cells was evaluated by measuring the elevated $[Ca^{2+}]o$-dependent inhibition of cyclic AMP accumulation, induced by either prostaglandin E_2 or forskolin. Elevated $[Ca^{2+}]o$ stabilized expression of cyclin D1, a protein required for cell cycle transition. Furthermore, elevated $[Ca^{2+}]o$ triggered activation of the Akt signaling pathway and enhanced PC-3 cell attachment. Both pertussis toxin (a G-protein inhibitor) and LY294002 (an inhibitor of Akt signaling) reduced cell attachment. These data suggest that elevated $[Ca^{2+}]o$ following increased bone remodeling could facilitate metastatic localization of prostate cancer via the CaSR and the Akt signaling pathway. Taken together, $[Ca^{2+}]o$ is a candidate mediator of prostate cancer bone metastasis. (Cancer Res 2006; 66(18): 9065-73)

Introduction

Prostate cancer is the second leading cause of cancer-associated mortality in American men, causing >30,000 deaths each year in United States (1). Although patients with localized prostate cancer can survive long periods of time, a large percent of diagnosed prostate cancer patients develop skeletal metastases. With the progression of skeletal metastasis, prostate cancer patients suffer a variety of complications, such as bone pain, fractures, spinal cord compression, and bone marrow suppression. The metastasis of prostate cancer to the skeleton dramatically lowers the patient's ability to maintain their usual activities and lifestyle and severely threatens their lives (2, 3).

Skeletal metastases of prostate cancer are found most frequently in the spine, followed by the femur, pelvis, rib cage, skull, and humerus (4, 5). These are bones that normally experience high rates of turnover. Bone turnover is continuous and relies on two opposite processes: bone formation and bone resorption. With an *in vivo* model, our laboratory and others have reported that prostate cancer preferentially localizes to skeletal sites with highly active bone turnover (3, 6, 7). Stimulation of bone turnover by parathyroid hormone (PTH) increased the localization of prostate cancer to the skeleton whereas inhibition of bone resorption by zoledronic acid, a potent inhibitor of osteoclast activity, suppressed skeletal lesions by prostate cancer cells (6, 7). Recently, it was reported that zoledronic acid also decreases the risk of skeletal complications in men with androgen-independent prostate cancer and bone metastases (8–10). These findings suggest that bone turnover facilitates the spread of prostate cancer to bone, but the mechanisms for this are as yet unclear.

During the process of bone turnover, organic and inorganic bioactive products are generated and released. Calcium is the main inorganic component. Normally, physiologic ionized calcium levels are kept within a narrow range of 1.1 to 1.3 mmol/L (11). In active bone resorptive lacunae, extracellular calcium ($[Ca^{2+}]o$) can reach levels as high as 8 to 40 mmol/L, whereas in the proximity of the nonresorbing bone surfaces, $[Ca^{2+}]o$ is $\sim$2 mmol/L (12, 13). $[Ca^{2+}]o$ is important for bone formation and physiologic homeostasis of a multitude of body functions. $[Ca^{2+}]o$ regulates proliferation, differentiation, and apoptosis, three important cellular processes that determine cell fate in addition to the regulation of cell migration (14). Hence, local elevation in the concentration of free ionized $[Ca^{2+}]o$ may influence the metastatic behavior of tumors.

$[Ca^{2+}]o$ functions mainly through the extracellular calcium-sensing receptor (CaSR; ref. 14). The CaSR is a heterotrimeric G-protein–coupled receptor, with at least 2 Gα subunits involved in its transmembrane signaling, Gαi and Gαq. Activation of the CaSR inhibits the generation of cyclic AMP (cAMP) and activates phospholipase C to produce inositol 1,4,5-triphosphate (15, 16). It has also been reported that protein kinase C, extracellular signal–regulated kinase (ERK), p38, and Akt are involved in the intracellular signaling (17–20). Expression of the CaSR is found in many normal tissues including parathyroid, kidney, skeleton, intestine, heart, as well as malignant tissues, such as breast cancer and colorectal cancer (14, 21–24). CaSR mRNA and protein expression have also been identified in human-derived prostate cancer cell lines (25) and microarray data have suggested that expression of the CaSR is associated with prostate cancer metastatic behavior (26). Nevertheless, it still remains unclear what the role of $[Ca^{2+}]o$ is in the microenvironment of the prostate carcinoma lesion in bone. The purpose of this study was to determine the effects of $[Ca^{2+}]o$ on prostate cancer cell proliferation and attachment via signaling through the CaSR. These

Requests for reprints: Laurie K. McCauley, Department of Periodontics and Oral Medicine, School of Dentistry, University of Michigan, Room 3343, 1011 North University Avenue, Ann Arbor, MI 48109-1078. Phone: 734-647-3206; Fax: 734-763-5503; E-mail: mccauley@umich.edu.

doi:10.1158/0008-5472.CAN-06-0317

studies will facilitate a better understanding of the role of $[Ca^{2+}]o$ in the pathophysiology of prostate cancer skeletal metastasis.

Materials and Methods

Cell lines and culture. LNCaP, C4-2B, PC-3, and PC-3 stably expressing luciferase (PC-3/Luc+; refs. 27–30) were maintained at 37°C and 5% CO_2 in RPMI 1640-10% fetal bovine serum (FBS) and 1% penicillin-streptomycin (Invitrogen Corp., Carlsbad, CA).

Reagents. pENTRTM/H1/TO vector, LipofectAMINE Plus reagents, Zeocin, and Trizol reagent were from Invitrogen. CHAPS was from U.S. Biochemical Corp. (Cleveland, OH). The pharmacologic inhibitors LY294002, PD98059, and pertussis toxin were purchased from Calbiochem (San Diego, CA). Treatments with pharmacologic inhibitors were done 30 minutes before challenge. Rabbit anti-Akt, pAkt (Ser^{473}), ERK, and pERK antibodies were obtained from Cell Signaling Technology, Inc. (Beverly, MA). Rabbit anti-CaSR antibody was from Abcam Ltd. (Cambridge, MA). Mouse anti-cyclin D1 was obtained from Santa Cruz Biotechnology (Santa Cruz, CA). Mouse anti-α-tubulin antibody, forskolin, prostaglandin E_2 (PGE_2), isobutylmethylxanthine, and bovine serum albumin (BSA) were obtained from Sigma-Aldrich Co. (St. Louis, MO). [^{3}H]cAMP was purchased from ICN (Irvine, CA). The luciferase assay system was from Promega Corp. (Madison, WI).

Construction of CaSR short hairpin RNA. CaSR short hairpin RNA (shRNA) plasmid was constructed by inserting double-strand oligonucleotides, which contain the CaSR sequence (5′-GGAACTATTCCATCATCA-ACT-3′; accession no. NM_000388), into the pENTRTM/H1/TO vector per recommendations of the manufacturer. The plasmid construction was confirmed by DNA sequencing. As a control, a LacZ shRNA plasmid was constructed using the same vector and procedure.

Transfection and selection. All transfections were done with Lipofect-AMINE Plus reagents and their recommended protocol (Invitrogen). After transfection, Zeocin-resistant clones were selected with 800 μg/mL Zeocin. The expression of target genes was validated with Western blot analysis.

RT-PCR. Total RNA from different prostate cancer cell lines was isolated with Trizol reagent. The possible contamination of genomic DNA was avoided with Qiagen RNeasy mini kit (Qiagen, Inc., Valencia, CA) and treatment with DNase I. Total RNA (1 μg) was reverse transcribed in a 20-μL reaction volume containing random hexamers with a reverse transcription assay system (Roche Applied Sciences, Indianapolis, IN). Reverse transcription was done at 25°C for 10 minutes, 48°C for 30 minutes, and 95°C for 5 minutes. As a control, total RNA (1 μg) was treated with RNase before reverse transcription.

PCR primers were obtained from Invitrogen. The sequences of the primers were as follows: CaSR, 5′-TCAACCTGCAGTTCCTGCTGG-3′ (forward) and 5′-TGGCATAGGCTGGAATGAAGG-3′ (reverse; ref. 31); 28S rRNA, 5′-TTGAAAATCCGGGGGAGAG-3′ (forward) and 5′-ACATTGTTCCAA-CATGCCAG-3′ (reverse; ref. 32).

Adenylyl cyclase stimulation and cAMP assay. The adenylyl cyclase stimulation and cAMP-binding protein assays were done as previously described with minor modification (33). Cells were plated in triplicate at $2 \times 10^4/cm^2$ into 24-well plates. When cells became confluent, medium was replaced with 0.5 mL of calcium- and magnesium-free HBSS (Invitrogen) containing 0.1% BSA and 1 mmol/L isobutylmethylxanthine at 37°C for 15 minutes. PGE_2 (1 ng/mL) was added in the presence or absence of calcium or neomycin (a well-characterized CaSR agonist) for 15 minutes at 37°C. After aspirating the medium, cAMP was extracted by adding 250 μL/well ice-cold 5% perchloric acid and incubating overnight at 20°C. After thawing, the pH was adjusted to 7.5 with 4 N KOH, and the neutralized extract was then assayed for cAMP with a cAMP-binding protein assay. The cAMP-binding protein assay was done by incubating [^{3}H]cAMP with standards or unknowns and a cAMP-binding protein sufficient to bind ~30% of radioactivity for 90 minutes on ice. The samples were then incubated with dextran-coated charcoal for 20 minutes and centrifuged to remove unbound from bound cAMP-binding protein-[^{3}H]cAMP complexes. The radioactivity of the supernatants was determined with a liquid scintillation spectrophotometer and cAMP levels calculated by the log-logit method with the GraphPad Prism 3 program (GraphPad Software, San Diego, CA).

Viable cell enumeration assay. Prostate cancer cells were plated in triplicate in 24-well plates at a density of $10^4/cm^2$ in complete growth medium. The following day, medium was changed to Ca^{2+}-free DMEM (Invitrogen) supplemented with 1% FBS, 100 units/mL penicillin, 100 μg/mL streptomycin, and 2 mmol/L L-glutamine, which was either used alone or containing 0.5 mmol/L $CaCl_2$ (low concentration) or 2.5 mmol/L $CaCl_2$ (elevated concentration). Viable cell numbers were determined on indicated days by the trypan blue dye exclusion method with a hematocytometer as previously described (34). The cell enumeration assay for CaSR shRNA–expressing and control cells was done similarly, except refreshing with complete medium rather than with Ca^{2+}-free DMEM.

***In vivo* localization of PC-3 prostate cancer cells.** To evaluate the skeletal progression of prostate cancer, luciferase-positive PC-3 cells (LacZ control or CaSR shRNA) were inoculated into the left ventricle of male athymic mice (5-6 weeks old) as previously described (6). All experimental animal procedures were done in compliance with institutional ethical requirements and approved by the University of Michigan Committee for the Use and Care of Animals. *In vivo* bioluminescent imaging was carried out at the University of Michigan Small Animal Imaging Resource facility.[4] Before imaging, mice were injected i.p. with 100 μL of 40 mg/mL luciferin dissolved in PBS. Imaging was done under 1.75% isofluorane/air anesthesia on a cryogenically cooled IVIS system equipped with a 50-mm lens and coupled to a data acquisition PC running LivingImage software (Xenogen Corp., Alameda, CA). Ventral images were acquired 12 minutes after injection. Pseudocolor images of photon emissions were overlaid on grayscale images of mice to aid in determining signal spatial distribution. Photon quantifications were calculated within regions of interest.

Cell attachment. PC-3/Luc+ prostate cancer cells were plated and cultured to exponential growth phase, trypsinized, enumerated, and resuspended in calcium-free DMEM containing 10% serum supplemented with indicated calcium concentrations and/or neomycin (300 μmo/L). Cells were then seeded at 2×10^4/0.5 mL/well in 24-well plates. Cells were incubated for 4 hours at 37°C and 5% CO_2. Following incubation, the unattached cells were rinsed away with PBS whereas the attached cells were lysed by adding 100 μL of 1× Passive Lysis Buffer (Promega). The luciferase activities were measured with the Promega luciferase assay system and a Monolight 2010 luminometer (Analytical Luminescence Laboratory).

Western blotting. Cells were washed in ice-cold 1× PBS, scraped, and pelleted by centrifugation (500 × *g*, 5 minutes). The cell pellet was resuspended for 15 minutes in 1× lysis buffer [20 mmol/L MOPS, 5 mmol/L $MgCl_2$, 0.1 mmol/L EDTA, 200 mmol/L sucrose (pH 7.4), containing 1% CHAPS and phosphatase and protease inhibitors]. Cell suspensions were centrifuged at 13,000 × *g* for 10 minutes to remove nuclei and cell debris. The protein concentration was determined by the method of Bradford. Lysates containing equal amounts of protein were separated by SDS-PAGE and transferred to polyvinylidene difluoride membrane (Bio-Rad Laboratories, Hercules, CA). The membrane was blocked with 5% nonfat milk in TBS-0.1% Tween 20. Blots were incubated with primary antibodies (1:1,000) for 2 to 3 hours at room temperature or overnight at 4°C. Following washing in TBS-0.1% Tween 20, blots were incubated with horseradish peroxidase–labeled secondary antibodies (1:10,000) for 1 hour at room temperature. After washing, the signals were detected by standard enhanced chemiluminescence. The signals were quantitated with background subtraction using a UMAX scanner and Scion image and normalized to untreated controls.

Statistical analysis. Student's *t* test for independent analysis or ANOVA was applied to evaluate differences with the GraphPad Instat software program. $P < 0.05$ was considered statistically significant. All assays were repeated at least twice with similar results.

[4] http://www.med.umich.edu/msair/.

Results

[Ca^{2+}]o stimulated prostate cancer cell growth. To explore whether calcium released during bone turnover may support prostate tumor growth, the effect of extracellular calcium on cell proliferation was observed with trypan blue viable cell count. PC-3, a highly tumorigenic and skeletal metastatic cell line (29), had increased cell numbers over time in the presence of elevated [Ca^{2+}]o (2.5 mmol/L) versus low [Ca^{2+}]o (0.5 mmol/L; Fig. 1). Cells cultured for 6 days in medium that contained elevated [Ca^{2+}]o showed a substantial increase in viable cell number at day 6 when compared with cells maintained in low [Ca^{2+}]o. Cell enumeration of LNCaP, a low tumorigenic and metastatic prostate cancer cell line, and its highly skeletal metastatic variant C4-2B were also determined (27, 28). In the presence of elevated [Ca^{2+}]o, C4-2B cell numbers increased similarly to PC-3. In contrast, LNCaP cells had similar cell numbers regardless of the [Ca^{2+}]o levels.

The CaSR is the major receptor on the cell membrane for sensing [Ca^{2+}]o and is present in normal tissue and many types of tumors (14, 21–24). Expression of the CaSR in prostate cancer cell lines was measured by RT-PCR. Total RNA from LNCaP, C4-2B, and PC-3 was evaluated for the expression of the CaSR and the specific RT-PCR products for CaSR (318 bp) and 28S RNA (100 bp) were clearly detected (Fig. 1*B*). The highest expression of CaSR was detected in C4-2B. Moderate expression of the CaSR was detected in PC-3 and minimal expression of CaSR was detected in LNCaP. Detection of CaSR protein in these prostate cancer cell lines was also determined. Similar to the RNA levels, C4-2B and PC-3 expressed detectable CaSR levels whereas LNCaP expressed much lower levels of CaSR protein (Fig. 1*C*).

Reduced expression of CaSR restricts PC-3 proliferation. The CaSR has been reported to mediate cell proliferation in normal and malignant cells, including osteoblasts, fibroblasts, astrocytoma, multiple myeloma, and testicular cancer (20, 35–38). Nevertheless, the role of the CaSR in prostate cancer has not been well characterized. To further validate the role of CaSR in the mitogenic effects of [Ca^{2+}]o, an RNA interference strategy was applied. A CaSR shRNA plasmid was stably transfected into PC-3 cells to reduce CaSR expression (Fig. 2*A*). There was a significant reduction in CaSR shRNA–transfected cell numbers over time as compared with a LacZ vector control cell line (Fig. 2*B*).

Reduced expression of the CaSR suppresses tumor progression. To characterize the role of the CaSR in prostate cancer progression, CaSR shRNA stable transfectant (n = 13) and LacZ control (n = 15) of PC-3/Luc+ cells were inoculated into the left ventricle of athymic mice. The localization and growth of tumor cells were determined with bioluminescent imaging. Localization of PC-3 cells was predominantly found at the craniofacial region. A representative bioluminescent imaging from each group is shown in Fig. 2*C*. The luciferase activity of PC-3 tumors at the craniofacial region was significantly lower in the CaSR shRNA–inoculated mice at the 3rd, 4th, and 5th week (Fig. 2*D*).

Activation of the CaSR receptor by elevated [Ca^{2+}]o or the CaSR agonist neomycin. The CaSR is a seven-transmembrane G-protein–coupled receptor. Elevated [Ca^{2+}]o results in activation

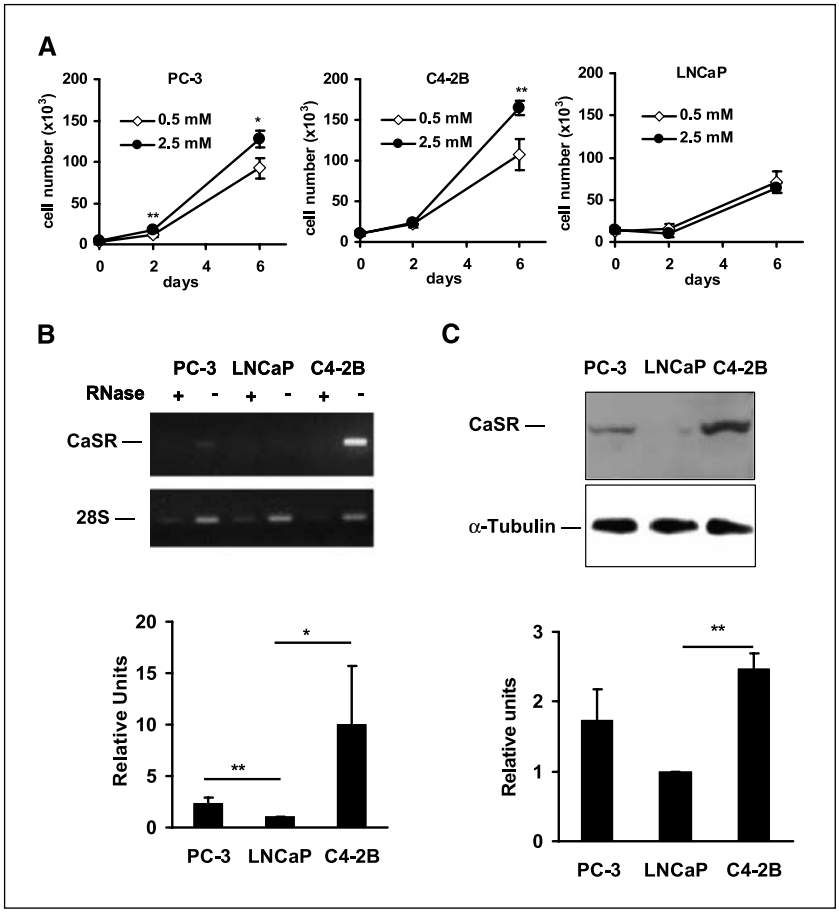

Figure 1. [Ca^{2+}]o promoted prostate cancer cell growth *in vitro. A,* prostate cancer cells were plated and the number of viable cells determined at the indicated times via trypan blue dye exclusion method. *, $P < 0.05$; **, $P < 0.01$, versus 0.5 mmol/L [Ca^{2+}]o at the same time point. *Points,* mean (n = 3 samples per group); *bars,* SE. *B,* total RNA was isolated from different prostate cancer cell lines, 1 μg was reverse transcribed, and the mRNA levels of CaSR were detected by PCR. RT-PCR product of 28S rRNA was used as an internal control for equal loading. RNase treatment of the RNA template was used to verify absence of genomic DNA contamination. *Top,* representative ethidium bromide–stained gel of RT-PCR. *Bottom,* plot of data from multiple RT-PCRs wherein signal intensity of CaSR versus 28S was quantified. *Columns,* mean (n = 4 samples per group); *bars,* SE. *, $P < 0.05$; **, $P < 0.01$, versus LNCaP. *C,* total proteins (100 μg) from cell lysates of different prostate cancer cell lines were applied to SDS-PAGE and blotted with a specific CaSR antibody. *Top,* representative Western blot of CaSR. *Bottom,* plot of data from multiple Western blot analyses wherein signal intensity of CaSR normalized to α-tubulin was quantified. *Columns,* mean (n = 3 samples per group); *bars,* SE. **, $P < 0.01$, versus LNCaP.

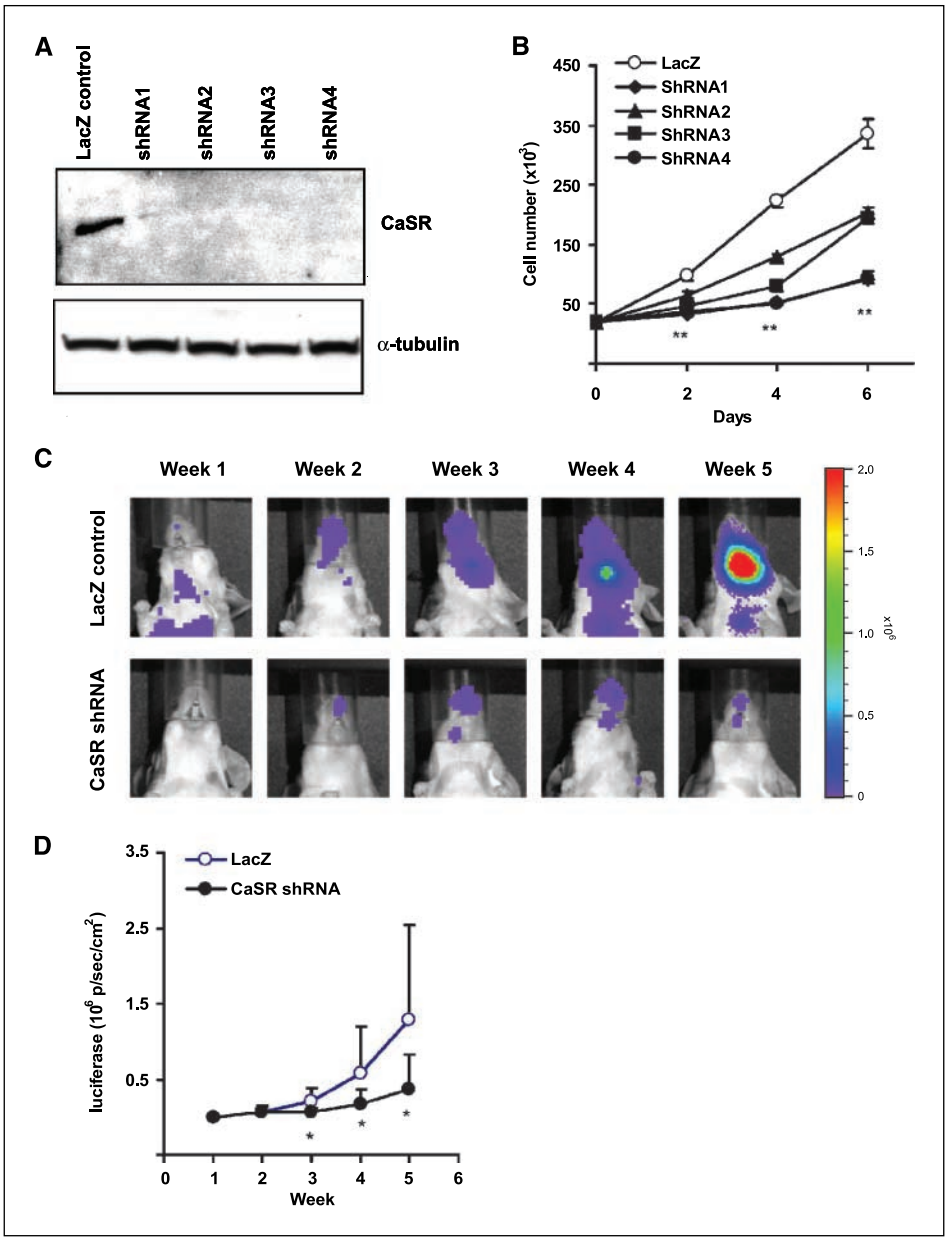

Figure 2. CaSR RNA interference. *A,* CaSR shRNA or LacZ vector control was stably transfected into PC-3/Luc+ cells and protein levels of CaSR were verified by Western blot. Reduced CaSR expression was found in PC-3/Luc+ cells with CaSR shRNA versus LacZ shRNA control. *B,* cell enumeration revealed CaSR shRNA transfectants had reduced numbers of cells over time. **, $P < 0.01$, CaSR shRNA groups versus LacZ control group. *C,* representative images of progression of PC-3/Luc+ cell in the craniofacial region. *D,* CaSR shRNA suppressed the growth of PC-3 cells in the craniofacial region. PC-3/Luc+ stable transfectants of CaSR shRNA and LacZ control were inoculated into left ventricle of athymic mice. Tumor localization and growth at the craniofacial region were determined by bioluminiscent imaging. Luciferase activity of tumors was measured as photons/s/cm^2. *, $P < 0.05$, CaSR shRNA ($n = 13$) versus LacZ control ($n = 15$).

of CaSR at the cell membrane. Activation of the CaSR, via either Gαi or Gαq, leads to the inhibition of adenylyl cyclase and, thus, an inhibition in the generation of cAMP (14). In the presence of 0.5 mmol/L [Ca^{2+}]o, PGE_2 significantly induced cAMP in PC-3 cells (Fig. 3*A*). This increase in cAMP in response to PGE_2 was significantly blocked in the presence of 2.5 mmol/L [Ca^{2+}]o. Neomycin, a CaSR agonist, also suppressed the accumulation of cAMP in response to PGE_2. Forskolin-induced cAMP elevation was also inhibited by elevated [Ca^{2+}]o (Fig. 3*B*).

[Ca^{2+}]o stabilized the expression of cyclin D1 in PC-3 cells. The expression of cyclin D1, a key component of cell cycle–mediated cell proliferation, was evaluated in PC-3 cells in response to increased levels of calcium. The level of cyclin D1 in PC-3 cells declined significantly when cells were maintained in 0.5 mmol/L [Ca^{2+}]o medium without serum. In contrast, the level of cyclin D1 in PC-3 cells did not decline at the same magnitude in the presence of 2.5 mmol/L [Ca^{2+}]o (Fig. 4*A* and *B*).

CaSR mediated [Ca^{2+}]o-dependent increase in prostate cancer cell attachment. Cell attachment is a critical step during the process of tumor metastasis. In PC-3 cells, cell attachment was significantly enhanced with higher [Ca^{2+}]o (Fig. 5*A*). Similarly, the CaSR agonist neomycin promoted the attachment of PC-3 cells (Fig. 5*B*). Pertussis toxin, a G-protein inhibitor that restricts CaSR signaling (39, 40), effectively decreased the attachment of

PC-3 cells in either elevated $[Ca^{2+}]o$ or neomycin-treated cultures (Fig. 5*C*).

CaSR mediated $[Ca^{2+}]o$-dependent increase in attachment via the Akt signaling pathway. Elevated $[Ca^{2+}]o$ triggers Akt and ERK signaling pathways, which are closely related to proliferation (20, 37, 38). The aberrant activation of these two signaling pathways in tumors are common. To elucidate the pathway that mediates the $[Ca^{2+}]o$-dependent increase in prostate cancer cell attachment, activation of Akt and ERK signaling pathways was evaluated. Figure 6*A* shows that activation of the CaSR with elevated $[Ca^{2+}]o$ significantly increased the active form of Akt (phospho-Akt) from 1 to 4 hours. Elevated $[Ca^{2+}]o$ (2.5 mmol/L) also caused a more rapid and transient activation of the ERK signaling pathway. The peak of the active ERK in response to $[Ca^{2+}]o$ was found at 5 minutes (Fig. 6*B*). Interestingly, blocking activation of phosphoinositide 3-kinase/Akt with the phosphoinositide 3-kinase inhibitor LY294002 inhibited the attachment of PC-3 cells. In contrast, pharmacologic inhibition of the ERK signaling pathway with PD98059 did not affect $[Ca^{2+}]o$-dependent increase of prostate cancer cell attachment (Fig. 6*C*).

Discussion

Prostate cancer characteristically spreads to skeletal sites (2, 3). The preferential localization and growth of prostate cancer cells in the skeleton indicates that the bone microenvironment provides a favorable niche for its growth. Multiple bone microenvironmental factors have been postulated to provide appropriate chemotaxis- and growth-promoting stimuli required for tumor localization and expansion (2, 41). $[Ca^{2+}]o$ is one of the major inorganic factors released during adult bone remodeling. The levels of $[Ca^{2+}]o$ in adults are stringently regulated and vary in a narrow range (1.1-1.3 mmol/L; ref. 11). However, in bones with active remodeling, specifically in the proximal ends of the long bones, ribs, and vertebral column, elevated $[Ca^{2+}]o$ exists. These regions are also the preferential sites of prostate cancer metastasis. Unlike other factors, the role of $[Ca^{2+}]o$ in facilitating the formation and growth of prostate cancer skeletal metastasis has been much more elusive. In the present study, the hypothesis that $[Ca^{2+}]o$ plays a role in supporting prostate cancer cell growth was tested.

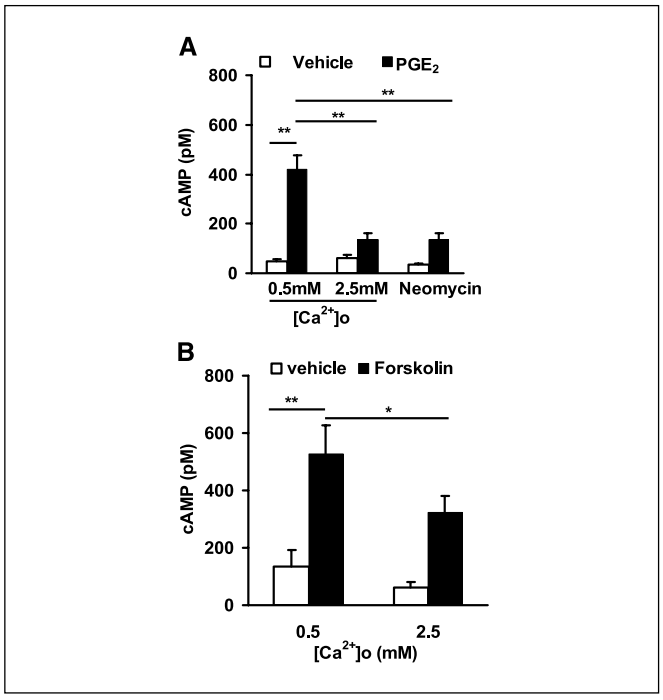

Figure 3. Activation of CaSR by calcium and neomycin in PC-3 cells. Activation of the CaSR was detected by the inhibition of either PGE_2- or forskolin-induced cAMP generation. PC-3 cells were cultured to confluence in 24-well plates and adenylyl cyclase stimulation was done in the presence of 0.5 and 2.5 mmol/L $[Ca^{2+}]o$ or neomycin (300 μmo/L) with PGE_2 (1 ng/mL; *A*) or forskolin (10 μmo/L; *B*). cAMP levels are expressed as picomolar concentrations. *Columns,* mean of triplicate samples; *bars,* SE. Representative of a minimum of two replicate assays. *, $P < 0.05$; **, $P < 0.01$.

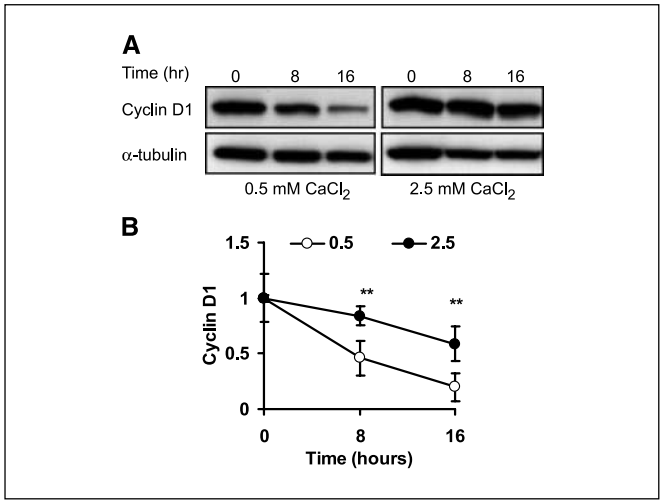

Figure 4. Elevated $[Ca^{2+}]o$ stabilized cyclin D1 expression in PC-3 cells. *A,* PC-3 cells were plated (70,000/cm^2) and, the next day, serum starved for 18 hours in basal medium containing 0.5 mmol/L $[Ca^{2+}]o$. The medium was then changed to 0.5 or 2.5 mmol/L $[Ca^{2+}]o$–containing, serum-free medium and whole-cell extracts were isolated at indicated time points. Representative Western blot. *B,* plot of data from Western blot analysis, normalized by α-tubulin. *Points,* mean ($n = 3$); *bars,* SE. Western blot analysis shows that cyclin D1 protein levels declined slightly but not significantly in the presence of 2.5 mmol/L $[Ca^{2+}]o$, whereas in cells cultured in 0.5 mmol/L $[Ca^{2+}]o$, cyclin D1 decreased significantly overtime. **, $P < 0.01$, versus 0.5 mmol/L $[Ca^{2+}]o$ at the same time point.

The effect of elevated $[Ca^{2+}]o$ on prostate cancer cell proliferation was investigated using three commonly used prostate cancer cell lines with different skeletal metastatic potentials. PC-3 is a prostate cancer cell line generated from a skeletal metastasis. It is highly tumorigenic and aggressive in animal models (29). LNCaP is a prostate cancer cell line isolated from lymph node. In animal models, LNCaP cells typically generate tumors when inoculated s.c., but do not result in metastasis. C4-2B is one of the androgen-independent variants of LNCaP and is capable of metastasizing to bone (27, 28). The data showed that elevated $[Ca^{2+}]o$ significantly promoted the proliferation of PC-3 and C4-2B cells, but not LNCaP.

Elevation of $[Ca^{2+}]o$ is mainly sensed by its cognate receptor, the CaSR (14). In this report, higher CaSR mRNA and protein expression was found in PC-3 and C4-2B cells as compared with LNCaP cells. CaSR expression in prostate cancer cells was correlated with the proliferative effect of elevated $[Ca^{2+}]o$ and the cellular metastatic behavior. The activation of CaSR by elevated $[Ca^{2+}]o$ was further confirmed in PC-3 cells. The CaSR is a heterotrimeric G-protein–coupled receptor. Through Gαi, high $[Ca^{2+}]o$ induces inhibition of cAMP accumulation in parathyroid cells and HEK293 cells stably transfected with the CaSR (42, 43). In the present study, PGE_2 and forskolin, as agonists, significantly

stimulated the generation of cAMP. Elevated $[Ca^{2+}]o$ dramatically suppressed either the PGE_2- or forskolin-triggered increase of cAMP. Neomycin, a well-characterized CaSR agonist, had a similar inhibitory effect on PGE_2-initiated cAMP generation. Furthermore, interference in CaSR signaling by pertussis toxin clearly prevented the CaSR-mediated increase in cell attachment. This suggests that the CaSR is a mediator of $[Ca^{2+}]o$-initiated effects on prostate cancer cells.

To investigate roles of $[Ca^{2+}]o$ and its receptor (CaSR) in prostate cancer skeletal progression, a RNA interference strategy was applied. CaSR shRNA effectively decreased expression of the CaSR in PC-3/Luc+ cells to ~10% to 60% of control cells at the protein level. Consistently, cell lines with reduced CaSR level by shRNA showed significantly slower proliferation *in vitro.* An intracardiac injection model was adopted to evaluate the involvement of the CaSR in prostate cancer skeletal metastasis. In this model, PC-3/Luc+ cells (either LacZ control or CaSR shRNA) were inoculated into the left ventricle of 5- to 6-week-old male athymic nude mice. Tumor localization and growth were tracked by bioluminescent imaging weekly. The craniofacial region is the predominant area where PC-3/Luc+ prostate cancer cells localize and expand rapidly (6). After 5 weeks, 8 of 15 mice that were injected with lacZ control PC-3/Luc+ cells developed evident metastasis at the craniofacial region. The luciferase activities at this region in these eight LacZ control mice were $>10^6$ photons/s/cm^2 and at least three-fold of the background. In contrast, only one mouse of the CaSR shRNA group showed luciferase activity $>10^6$ photons/s/cm^2 at this region. This suggests that *in vivo* growth of PC-3/Luc+ cells was significantly lowered by CaSR shRNA. Taken together, these data strongly support that the CaSR plays a role in facilitating prostate cancer expansion by promoting tumor proliferation.

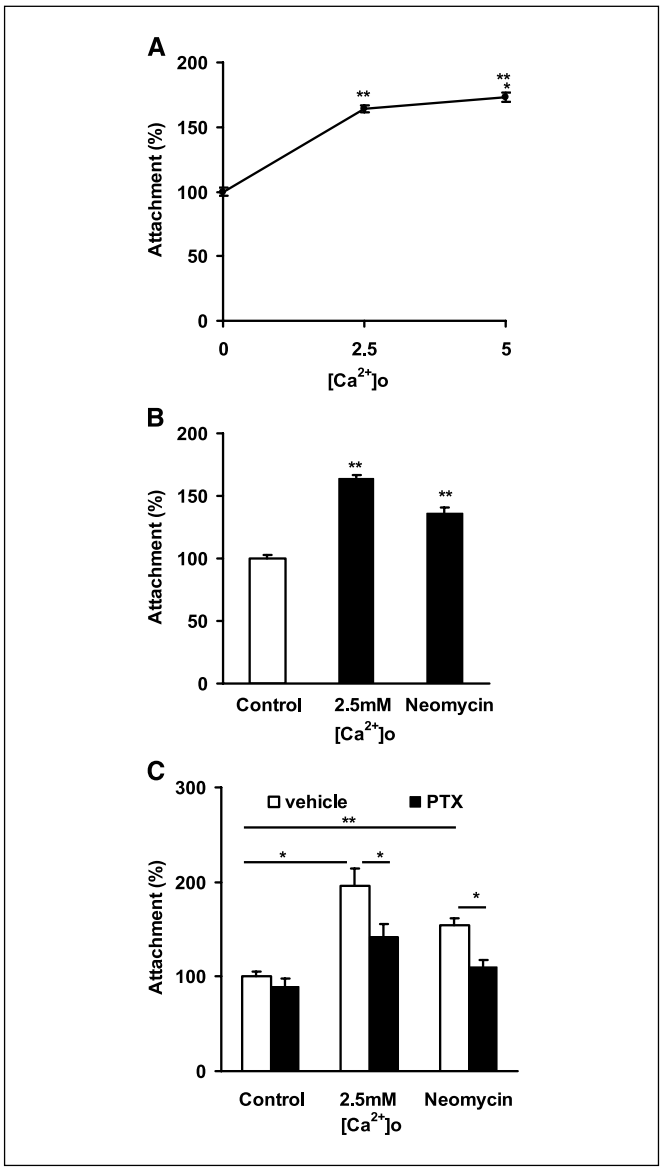

Figure 5. Activation of CaSR enhanced attachment of PC-3 cells. Cell attachment was determined in PC-3/Luc+ cells by evaluating luciferase activity of adherent cell monolayers 4 hours after plating. *A,* dose response of $[Ca^{2+}]o$ showing that increased $[Ca^{2+}]o$ promotes cell attachment. *Points,* mean of triplicate samples; *bars,* SE; treatment is expressed as a percent of control, and control is set at 100%. *, $P < 0.05$; **, $P < 0.01$, versus group without $[Ca^{2+}]o$. *B,* neomycin mimics $[Ca^{2+}]o$-mediated increase in cell attachment. Data expressed as in (*A*). **, $P < 0.01$. *C,* pertussis toxin (*PTX*) suppressed the attachment of prostate cancer cells. Data expressed as in (*A*). *, $P < 0.05$; **, $P < 0.01$.

The mitogenic effect of $[Ca^{2+}]o$ is consistent with recent studies showing similar findings in other CaSR-expressing tumor cells (20, 37, 38). Elevated $[Ca^{2+}]o$ in the range of 2.5 to 7.5 mmol/L, as well as CaSR agonists, induces cell proliferation when compared with low $[Ca^{2+}]o$ (0.5 mmol/L)–treated cells. The signaling mechanism of the $[Ca^{2+}]o$-triggered mitogenic effect is still controversial. Reports suggest it could be mediated by p38 mitogen-activated protein kinase (MAPK) or cross-activation of epidermal growth factor receptor/ERK signaling (20, 36). Because cell proliferation relies on the progression of cell cycle, $[Ca^{2+}]o$ may exert its mitogenic effect through regulation of cell cycle proteins. Using Western blot analysis, we found that elevated $[Ca^{2+}]o$ stabilized cyclin D1 expression under serum-free conditions. These findings suggest that elevated $[Ca^{2+}]o$ is a mitogenic factor for prostate cancer growth in bone.

Tumor cell attachment to extracellular matrix is a critical step in the spread of cancer (44). The current study provides evidence that elevated $[Ca^{2+}]o$ enhanced attachment of prostate cancer cells expressing CaSR. Neomycin, a well-characterized CaSR agonist, had a similar effect, validating the CaSR as a key component in the mechanism. Pertussis toxin, a G-protein inhibitor, reduced the increase induced by elevated $[Ca^{2+}]o$ or neomycin. A recent report showed that the CaSR is essential for hemopoietic cell adherence to collagen, which is the most prominent extracellular matrix protein in bone (45). Hence, data from the present study and other reports suggest that $[Ca^{2+}]o$ could play an important role not only in stimulating growth but also in early stages of prostate cancer localization to bone.

Akt is an antiapoptotic molecule and is also involved in proliferation and adhesion/migration (46). Elevation of Akt phosphorylation at Ser^{473} is very common in malignant prostate cancer and other malignant tumors (47). Alterations of the Akt signaling pathway are closely associated with tumorigenesis and progression (47). The present study also showed that elevated $[Ca^{2+}]o$ induced activation of both ERK and Akt signaling pathways. The activation of ERK signaling pathway by elevated $[Ca^{2+}]o$ was rapid and transient. In contrast, the active Akt (pAkt-Ser^{473}) started later and remained stable up to 4 hours. Because inhibition of the Akt signaling pathway by the phosphoinositide 3-kinase inhibitor (LY294002) decreased the $[Ca^{2+}]o$-mediated increase in cell attachment, it seems that Akt, but not ERK, is

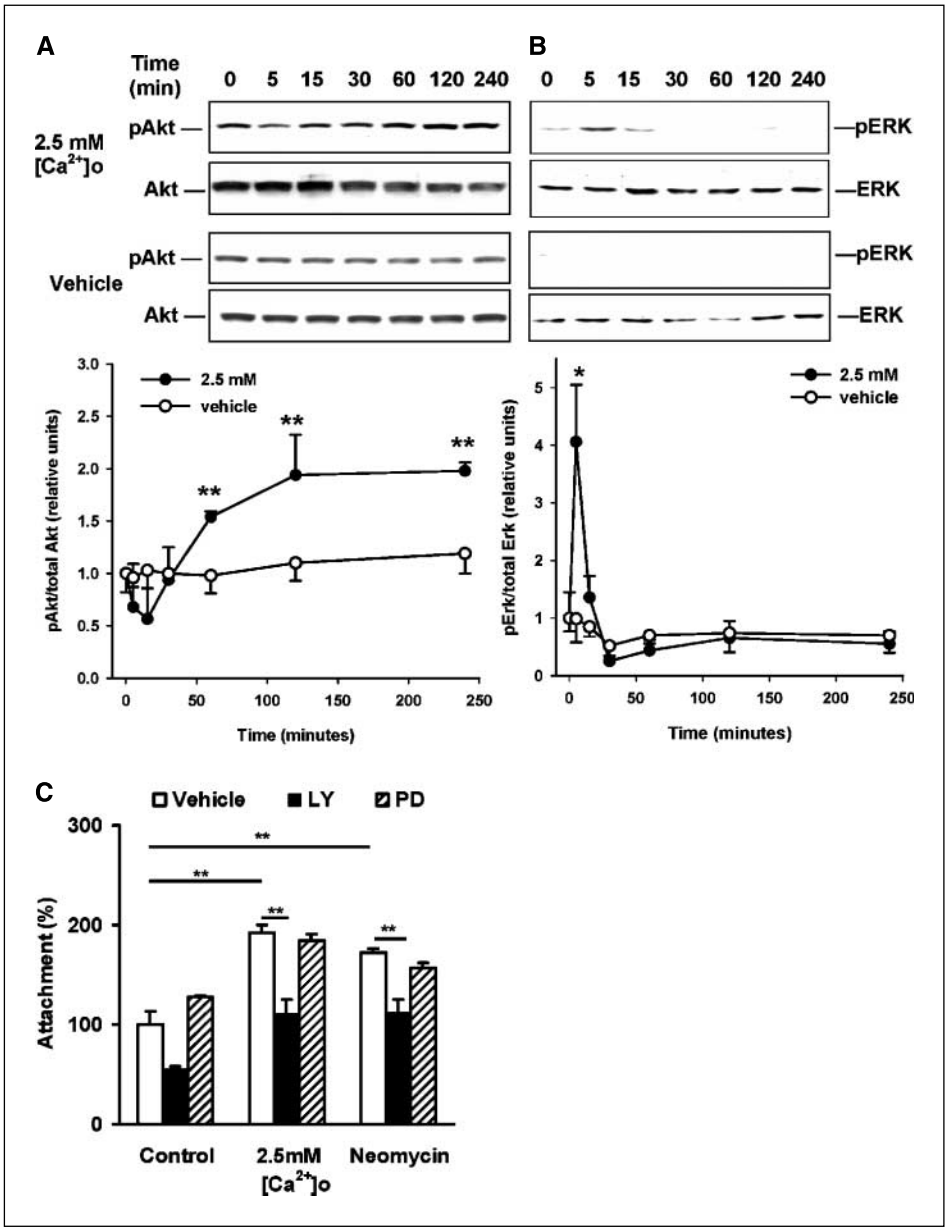

Figure 6. $[Ca^{2+}]o$ activates Akt and ERK signaling pathways in PC-3 cells. *A,* elevated $[Ca^{2+}]o$ stimulated Akt phosphorylation. PC-3 cells were plated in complete growth medium and, the next day, serum starved for 18 hours in calcium-free DMEM containing 0.5 mmol/L $[Ca^{2+}]o$. Following this period, 2.5 mmol/L $[Ca^{2+}]o$ or vehicle control was added, and at the indicated time points the whole-cell extracts were isolated. *Top,* Western blot analysis showed a time-dependent increase in Akt phosphorylation at Ser^{473} (pAkt-Ser^{473}) in response to 2.5 mmol/L $[Ca^{2+}]o$. Representative Western blot image. *Bottom,* plot of data from Western blot analysis. *Points,* mean ($n = 4$); *bars,* SE. **, $P < 0.01$, versus time point 0. *B,* cells were plated and treated as in (*A*). *Top,* Western blot analysis showed an increase in ERK phosphorylation in response to 2.5 mmol/L $[Ca^{2+}]o$. Representative Western blot image. *Bottom,* plot of data from Western blot analysis. *Points,* mean ($n = 4$); *bars,* SE. **, $P < 0.01$, versus time point 0. *C,* inhibition of phosphoinositide 3-kinase/Akt, but not ERK, signaling pathway suppressed $[Ca^{2+}]o$-mediated increase of attachment in PC-3 cells. The attachment of PC-3 cells was determined as described in Fig. 5 in the presence of either phosphoinositide 3-kinase inhibitor LY294002 (*LY*; 20 μmo/L) or MAPK inhibitor PD98059 (*PD*; 40 μmo/L). *Columns,* mean ($n = 3$); *bars,* SE. **, $P < 0.01$.

involved in the $[Ca^{2+}]o$-mediated increase in cell attachment. It follows that Akt could be an important target of $[Ca^{2+}]o$ actions during the establishment of prostate cancer skeletal metastasis.

Although the major mechanisms of bone metastasis still remain poorly understood, the interaction between tumor and bone cannot be underestimated. Parathyroid hormone–related peptide (PTHrP) is a peptide that binds the same PTH/PTHrP receptor as PTH and is similar in promoting bone resorption. PTHrP is commonly overexpressed in multiple tumors with skeletal metastasis (48). Previously, we reported that PC-3 prostate cancer cells, when injected into left ventricle of nude mice, preferred to localize at the hind limb and craniofacial regions. PTH administration enhanced this skeletal localization (6). A recent report presented evidence that ectopic expression of PTHrP converted noninvasive prostate cancer cells into ones that caused skeletal progression (49). Consistently, several reports showed that inhibition of osteoclastic activity and bone resorption prevented bone metastasis and skeletal lesions by prostate cancer (6–10).

Interestingly, a recent clinical study reported that higher levels of serum PTH were significantly and negatively associated with survival in androgen-independent prostate cancer (50). A feedback loop between CaSR and PTHrP exists. In prostate cancer and breast cancer, elevated-[Ca^{2+}]o stimulates PTHrP secretion (18, 22, 25). The findings in the present study therefore suggest that the PTHrP-[Ca^{2+}]o-CaSR axis may act as a potential mechanism to facilitate and further support prostate cancer localization and growth in the skeleton. Prostate cancer cells manipulate the bone microenvironment by PTHrP production and the subsequent release of ionized [Ca^{2+}]o, as well as through other factors. The CaSR in prostate cancer cells, therefore, senses the change in [Ca^{2+}]o and provides signals to facilitate the ability of cancer to thrive in the skeleton. The interaction may be critical for prostate cancer skeletal metastasis and associated complications. Taken together, the current study supports [Ca^{2+}]o as a mediator of prostate cancer pathophysiology.

Disrupting the tumor-bone interaction by targeting both tumor and bone microenvironment could lead to novel, effective therapeutic approaches. Indeed, antagonizing the tumor cell CaSR with calcilytic drugs that prevent its activation in conjunction with antiresorptive agents, such as bisphosphonates, may result in a novel therapeutic approach to control both osteolysis and tumor cell proliferation. Further studies are warranted to gain more insight into the specific role of high [Ca^{2+}]o and, in particular, the CaSR in mediating tumor cell proliferation in skeletal metastasis.

Acknowledgments

Received 1/26/2006; revised 6/27/2006; accepted 7/14/2006.

The costs of publication of this article were defrayed in part by the payment of page charges. This article must therefore be hereby marked *advertisement* in accordance with 18 U.S.C. Section 1734 solely to indicate this fact.

The authors acknowledge Dan Hall for his expert advice on bioluminescent imaging.

References

1. Nelson WG, De Marzo AM, Isaacs WB. Prostate cancer. N Engl J Med 2003;349:366–81.
2. Roodman GD. Mechanisms of bone metastasis. N Engl J Med 2004;350:1655–64.
3. Mundy GR. Metastasis to bone: causes, consequences and therapeutic opportunities. Nat Rev Cancer 2002;2:584–93.
4. Imbriaco M, Larson SM, Yeung HW, et al. A new parameter for measuring metastatic bone involvement by prostate cancer: the bone scan index. Clin Cancer Res 1998;4:1765–72.
5. Roudier MP, True LD, Higano CS, et al. Phenotypic heterogeneity of end-stage prostate carcinoma metastatic to bone. Hum Pathol 2003;34:646–53.
6. Schneider A, Kalikin LM, Mattos AC, et al. Bone turnover mediates preferential localization of prostate cancer in the skeleton. Endocrinology 2005;146:1727–36.
7. Miwa S, Mizokami A, Keller ET, Taichman R, Zhang J, Namiki M. The bisphosphonate YM529 inhibits osteolytic and osteoblastic changes and CXCR-4-induced invasion in prostate cancer. Cancer Res 2005;65:8818–25.
8. Clezardin P, Ebetina FH, Fournier PG. Bisphosphonates and cancer-induced bone disease:beyond their antiresorptive activity. Cancer Res 2005;65:4971–4.
9. Smith MR. Zoledronic acid to prevent skeletal complications in cancer: corroborating the evidence. Cancer Treat Rev 2005;31 Suppl 3:19–25.
10. Michaelson MD, Smith MR. Bisphosphonates for treatment and prevention of bone metastases. J Clin Oncol 2005;23:8219–24.
11. Dvorak MM, Siddiqua A, Ward DT, et al. Physiological changes in extracellular calcium concentration directly control osteoblast function in the absence of calciotropic hormones. Proc Natl Acad Sci U S A 2004;101:5140–5.
12. Berger CE, Rathod H, Gillespie JI, Horrocks BR, Datta HK. Scanning electrochemical microscopy at the surface of bone-resorbing osteoclasts: evidence for steady-state disposal and intracellular functional compartmentalization of calcium. J Bone Miner Res 2001;16:2092–102.
13. Silver IA, Murrills RJ, Etherington DJ. Microelectrode studies on the acid microenvironment beneath adherent macrophages and osteoclasts. Exp Cell Res 1988;175:266–76.
14. Brown EM, MacLeod RJ. Extracellular calcium sensing and extracellular calcium signaling. Physiol Rev 2001;81:239–97.
15. Kifor O, Diaz R, Butters R, Brown EM. The Ca^{2+}-sensing receptor (CaR) activates phospholipases C, A2, and D in bovine parathyroid and CaR-transfected, human embryonic kidney (HEK293) cells. J Bone Miner Res 1997;12:715–25.
16. Hawkins D, Enyedi P, Brown EM. The effects of high extracellular Ca^{2+} and Mg^{2+} concentrations on the levels of inositol 1,3,4,5-tetrakisphosphate in bovine parathyroid cells. Endocrinology 1989;124:838–44.
17. Kifor O, Diaz R, Butters R, Kifor I, Brown EM. The calcium-sensing receptor is localized in caveolin-rich plasma membrane domains of bovine parathyroid cells. J Biol Chem 1998;273:21708–13.
18. Yano S, Macleod RJ, Chattopadhyay N, et al. Calcium-sensing receptor activation stimulates parathyroid hormone-related protein secretion in prostate cancer cells: role of epidermal growth factor receptor transactivation. Bone 2004;35:664–72.
19. Tfelt-Hansen J, MacLeod RJ, Chattopadhyay N, et al. Calcium-sensing receptor stimulates PTHrP release by pathways dependent on PKC, p38 MAPK, JNK, ERK1/2 in H-500 cells. Am J Physiol Endocrinol Metab 2003;285:E329–37.
20. Tfelt-Hansen J, Chattopadhyay N, Yano S, et al. Calcium-sensing receptor induces proliferation through p38 mitogen-activated protein kinase and phosphatidylinositol 3-kinase but not extracellularly regulated kinase in a model of humoral hypercalcemia of malignancy. Endocrinology 2004;145:1211–7.
21. Cheng I, Klingensmith ME, Chattopadhyay N, et al. Identification and localization of the extracellular calcium-sensing receptor in human breast. J Clin Endocrinol Metab 1998;83:703–7.
22. Sanders JL, Chattopadhyay N, Kifor O, Yamaguchi T, Butters RR, Brown EM. Extracellular calcium-sensing receptor expression and its potential role in regulating parathyroid hormone-related peptide secretion in human breast cancer cell lines. Endocrinology 2000;141:4357–64.
23. Sheinin Y, Kallay E, Wrba F, Kriwanek S, Peterlik M, Cross HS. Immunocytochemical localization of the extracellular calcium-sensing receptor in normal and malignant human large intestinal mucosa. J Histochem Cytochem 2000;48:595–602.
24. Chakrabarty S, Radjendirane V, Appelman H, Varani J. Extracellular calcium and calcium sensing receptor function in human colon carcinomas: promotion of E-cadherin expression and suppression of β-catenin/TCF activation. Cancer Res 2003;63:67–71.
25. Sanders JL, Chattopadhyay N, Kifor O, Yamaguchi T, Brown EM. Ca($^{2+}$)-sensing receptor expression and PTHrP secretion in PC-3 human prostate cancer cells. Am J Physiol Endocrinol Metab 2001;281:E1267–74.
26. Dhanasekaran SM, Barrette TR, Ghosh D, et al. Delineation of prognostic biomarkers in prostate cancer. Nature 2001;412:822–6.
27. Wu HC, Hsieh JT, Gleave ME, Brown NM, Pathak S, Chung LW. Derivation of androgen-independent human LNCaP prostatic cancer cell sublines: role of bone stromal cells. Int J Cancer 1994;57:406–12.
28. Thalmann GN, Anezinis PE, Chang SM, et al. Androgen-independent cancer progression and bone metastasis in the LNCaP model of human prostate cancer. Cancer Res 1994;54:2577–81.
29. Kaighn ME, Narayan KS, Ohnuki Y, Lechner JF, Jones LW. Establishment and characterization of a human prostatic carcinoma cell line (PC-3). Invest Urol 1979;17:16–23.
30. Kalikin LM, Schneider A, Thakur MA, et al. *In vivo* visualization of metastatic prostate cancer and quantitation of disease progression in immunocompromised mice. Cancer Biol Ther 2003;2:656–60.
31. Jung SY, Kwak JO, Kim HW, et al. Calcium sensing receptor forms complex with and is up-regulated by caveolin-1 in cultured human osteosarcoma (Saos-2) cells. Exp Mol Med 2005;37:91–100.
32. Xu SW, Howat SL, Renzoni EA, et al. Endothelin-1 induces expression of matrix-associated genes in lung fibroblasts through MEK/ERK. J Biol Chem 2004;279:23098–103.
33. McCauley LK, Rosol TJ, Merryman JI, Capen CC. Parathyroid hormone-related protein binding to human T-cell lymphotropic virus type I-infected lymphocytes. Endocrinology 1992;130:300–6.
34. Chen HL, Demiralp B, Schneider A, et al. Parathyroid hormone and parathyroid hormone-related protein exert both pro- and anti-apoptotic effects in mesenchymal cells. J Biol Chem 2002;277:19374–81.
35. Chattopadhyay N, Yano S, Tfelt-Hansen J, et al. Mitogenic action of calcium-sensing receptor on rat calvarial osteoblasts. Endocrinology 2005;145:3451–62.
36. Tomlins SA, Bollinger N, Creim J, Rodland KD. Cross-talk between the calcium-sensing receptor and the epidermal growth factor receptor in Rat-1 fibroblasts. Exp Cell Res 2005;308:439–45.
37. Yamaguchi T, Yamaguchi M, Sugimoto T, et al. The extracellular calcium (Ca_o^{2+})-sensing receptor is expressed in myeloma cells and modulates cell proliferation. Biochem Biophys Res Commun 2002;299:532–8.
38. Chattopadhyay N, Ye CP, Yamaguchi T, Kerner R, Vassilev PM, Brown EM. Extracellular calcium-sensing receptor induces cellular proliferation and activation of a nonselective cation channel in U373 human astrocytoma cells. Brain Res 1999;851:116–24.
39. Holstein DM, Berg KA, Leeb-Lundberg LM, Olson MS, Saunders C. Calcium-sensing receptor-mediated ERK1/2 activation requires Gαi2 coupling and dynamin-independent receptor internalization. J Biol Chem 2004;279:10060–9.
40. Godwin SL, Soltoff SP. Calcium-sensing receptor-mediated activation of phospholipase C-γ1 is downstream of phospholipase C-β and protein kinase C in MC3T3-1 osteoblasts. Bone 2002;30:559–66.

41. Clines GA, Guise TA. Hypercalcaemia of malignancy and basic research on mechanisms responsible for osteolytic and osteoblastic metastasis to bone. Endocr Relat Cancer 2005;12:549–83.
42. Chen C, Barnett J, Congo D, Brown E. Divalent cations suppress 3′,5′-adenosine monophosphate accumulation by stimulating a pertussis toxin-sensitive guanine nucleotide-binding protein in cultured bovine parathyroid cells. Endocrinology 1989;124:233–9.
43. Chang W, Pratt S, Chen TH, Nemeth E, Huang Z, Shoback D. Coupling of calcium receptors to inositol phosphate and cyclic AMP generation in mammalian cells and *Xenopus laevis* oocytes and immunodetection of receptor protein by region-specific antipeptide antisera. J Bone Miner Res 1998;13:570–80.
44. Hood JD, Cheresh DA. Role of intergrins in cell invasion and migration. Nat Rev Cancer 2002;2:91–100.
45. Adam GB, Chabner KT, Alley IR, et al. Stem cell engraftment at the endosteal niche is specified by the calcium-sensing receptor. Nature 2006;439: 599–603.
46. Cheng JQ, Lindsley CW, Cheng GZ, Yang H, Nicosia SV. The Akt/PKB pathway: molecular target for cancer drug discovery. Oncogene 2005;24:c7482–92.
47. Majumder PK, Sellers WR. Akt-regulated pathways in prostate cancer. Oncogene 2005;24:7465–74.
48. McCauley LK, Schneider A. PTHrP and skeletal metastasis. Cancer Treat Res 2004;118:125–47.
49. Deftos LJ, Barken I, Burton DW, Hoffman RM, Geller J. Direct eveidence that PTHrP expression promotes prostate cancer progression in bone. Biochem Biophys Res Commun 2005;327:468–72.
50. Schwartz GG, Hall MC, Stindt D, Patton S, Lovato J, Torti FM. Phase I/II study of 19-nor-1α-25-dihydroxyvitamin D2 (paricalcitol) in advanced, androgen-insensitive prostate cancer. Clin Cancer Res 2005;11:8680–5.